FISEVIER

Contents lists available at ScienceDirect

### Journal of the Mechanical Behavior of Biomedical Materials

Journal of the Mechanical Behavior of Biomedical Materials

journal homepage: www.elsevier.com/locate/jmbbm

## Patient-specific mechanical analysis of PCL periodontal membrane: Modeling and simulation

Rakesh Pemmada <sup>a,1</sup>, Vicky Subhash Telang <sup>b,1</sup>, Puneet Tandon <sup>b,\*\*</sup>, Vinoy Thomas <sup>a,c,\*</sup>

- a Department of Mechanical and Materials Engineering, University of Alabama at Birmingham, United States
- b Department of Mechanical Engineering, PDPM Indian Institute of Information Technology Design and Manufacturing, Jabalpur, India
- <sup>c</sup> Department of Biomedical Engineering, University of Alabama at Birmingham, United States

#### ARTICLE INFO

# Keywords: Mechanical analysis Maxilla-scaffold Mandible-scaffold Finite elemental analysis (FEA) Load distribution

#### ABSTRACT

This research fills a knowledge gap in bone tissue engineering by examining the mechanical characteristics of scaffolds at bone-tissue interfaces utilizing a cutting-edge technique involving the creation of 3D scaffolds from Polycaprolactone (PCL). The work employs Finite element analysis to measure the scaffolds' maximum principal and Von Mises stresses and strains. CT scans of the Maxilla and Mandible were used to apply load conditions to 3D models of the upper central incisor. In the derived computational model, four different load situations considered were: the masticatory load (70–100 N at 45°), two parafunctional habits (100–130 N) and 500–550 N at the incisal edge, both at 45°), and a trauma case (800–850 N applied perpendicularly from the inwards direction at 90°). The findings revealed that the central tooth region experiences the highest stress concentration, while the Maxilla and Mandible regions show the least stress. These results provide critical insights into the mechanical behavior of scaffolds at bone-tissue interfaces, suggesting a research direction for developing scaffolds that closely mimic real bone characteristics. The results of this study are particularly significant for using bone replacement materials, providing an approach to more effective healing options for bone traumas and degenerative bone disorders.

#### 1. Introduction

Periodontal disease, a prevalent global affliction, is a chronic inflammatory condition targeting the foundational structures of our teeth, the gums, the periodontal ligament, and the alveolar bone (Cancedda et al., 2007). If untreated, its invasive nature poses a silent threat of tooth loss. Traditional interventions, notably scaling and root planning, though effective, are often dreaded by patients due to their invasive nature and associated discomfort (Lacroix and Prendergast, 2002). Facing the limitations of traditional treatments, the medical community is gravitating towards tissue engineering, a promising alternative that utilizes polycaprolactone (PCL) for periodontal repair due to its ideal combination of biocompatibility, biodegradability, and mechanical resilience (Dwivedi et al., 2020), (Bottino et al., 2011). The success of PCL implants, however, is deeply intertwined with their ability to foster cellular activities adhesion, proliferation, and differentiation essential

for tissue regeneration (Marei et al., 2009). These implants transcend their structural roles, actively catalyzing the regenerative processes necessary for healing periodontal tissues (Fallah et al., 2022). Thus, PCL is not merely a scaffold but an integral conductor in the intricate symphony of periodontal restoration (Choi et al., 2020). Modeling and simulation are not only effective but also economical and efficient, which makes them ideal for investigating distinctive design possibilities and boosting the efficacy and security of periodontal implant procedures. Such innovative methods allow us to examine the interaction between the implant and tissue in detail, providing us with important insights that were previously unattainable (Yoon et al., 2020). Therefore, modeling and simulation techniques help to advance the effectiveness of periodontal implant treatments. The development of scaffolds with a high compressive modulus has emerged as a significant area of interest in bone tissue engineering (Anjum et al., 2022). The mechanical strength of scaffold systems is crucial as it prevents the loss

<sup>\*</sup> Corresponding author. Department of Mechanical Engineering, University of Alabama, Birmingham, AL, United States.

<sup>\*\*</sup> Corresponding author. Mechanical Engineering Discipline, PDPM IIITDM, Jabalpur, M.P., India.

\*\*E-mail addresses: rpemmada@uab.edu (R. Pemmada), vickytelang@iiitdmj.ac.in (V.S. Telang), ptandon@iiitdmj.ac.in (P. Tandon), vthomas@uab.edu (V. Thomas).

<sup>1</sup> These authors contributed equally

of function of the newly formed bones (Corrales et al., 2014). Additionally, it is of utmost importance to consider the behavior of scaffolds and the regenerated bone under applied physical stresses and to accurately predict the behavior of scaffolds under mechanical forces, computational modeling methods have been employed. Although the fundamental processes involved in bone tissue engineering are thoroughly understood by the research community, the mechanical aspects of scaffolds and newly formed bones are yet to be explored in detail (Szabadi, 1996). Though in vitro and in vivo studies can evaluate various aspects of scaffold function, computational models can be of assistance in providing insights into how scaffolds may respond to mechanical forces encountered (Roseti et al., 2017). These forces may have a significant impact during the scaffold degradation process, where greater stresses are transferred to the newly formed bone (Bottino et al., 2012). Thus, the design and development of scaffolds with high compressive strength are critical in bone tissue engineering. Computational modeling methods can aid in accurately predicting scaffold behavior under mechanical forces and during degradation. It was realized that the study of mechanical aspects of scaffolds and newly formed bone is a promising area of research that requires further exploration (Gunn et al., 2021). Gautier et al. reviewed the intricate interaction between the biomechanics and structure of the periodontal ligament, emphasizing the difficulties in creating biomaterials for periodontal regeneration due to its mechanosensitivity and variable mechanical response under various loading circumstances (Gauthier et al., 2021). Fariha et al. devised an ibuprofen-functionalized nanofibrous membrane (IBU-PCL) for the treatment of periodontal disease. Its efficacy in lowering inflammation and accelerating wound healing was demonstrated both in vitro and in vivo, and it may provide a new strategy for improved periodontal regeneration (Batool et al., 2018). The current research utilized innovative methodology to investigate the stress distribution on the periodontal scaffolds placed at the Maxilla and Mandible under four different load conditions in a simulated 3D environment. This study is the first of its kind to provide a comprehensive analysis of the stress magnitude, direction, nature, and distribution dissipated in the scaffolds of specific Maxilla and Mandible regions due to occlusal load, thereby filling a significant gap in our understanding of this complex process. The findings of this work are expected to contribute to the development of more effective treatment strategies for dental issues, particularly those related to the Maxillary incisor tooth and periodontal tissues.

#### 2. Materials & methods

A study was conducted at the Polymers & Healthcare Materials and Devices lab at the University of Alabama, Birmingham, and the Indian Institute of Information Technology, Design and Manufacturing Jabalpur, India to create a modeling and finite element analysis (FEA)of a patient-specific diseased site. Obtaining Computerized Tomography (CT) images in Digital Imaging and Communications in Medicine (DICOM) format was the first step in the work. The imaging was performed with a CT scanner operating at 120 kV, 150 mA, 512  $\times$  512 matrix,  $14 \times 14$  cm field of view, and 0.5 mm slice thickness. As a result, a pixel size of 0.273 mm was produced. A patient who was 60 years of age volunteered to have CT images of the diseased site taken. During the imaging process, the patient followed the recommended guidelines. The CT images were 230 sections long along the axial axis obtained in a longitudinal direction for further analysis. The collection procedures, as well as the research methodology, were thorough and detailed, producing valuable data for future research in this area. An intricate procedure including numerous steps is required to create an accurate model for dental disease from DICOM images. To accomplish the objective at hand, this procedure makes use of SolidWorks, ANSYS workbench, 3D Slicer and Geomagic software and their algorithms. The process starts by acquiring CT scans from a CBCT scanner and subsequently saving the images in the DICOM format. Following this, the DICOM files are manually integrated into specialist visualization and processing tools. With the help of this feature, skilled clinicians can check and quantify numerous parameters at the oral diseased site.

Key parameters including lengths, angles, and spatial capabilities are essential in this process, where the key barriers involves effectively distinguishing the damaged tissue from the healthy surroundings in CT images. This key stage requires manual involvement to identify the impacted areas using advanced computational approaches such as thresholding or region-growing. Following segmentation, a coherent 3D model of the dental area is constructed, ensuring a comprehensive and detailed representation of the region of interest. Following that, clinicians assess the model and make any required modifications to allow for accurate planning of virtual treatments and simulations of procedures resultant 3D model is an asset for treatment planning and evaluation while also enabling virtual planning and simulation.

This work utilizes human derived CBCT scans, revealing the wide-spread manifestation of periodontal disease across multiple teeth in both the upper and lower jaws, particularly proximate to the Mandible and Maxilla. It was crucial to examine the precise locations across several teeth due to the multifocal nature of the disease presentation. As such, two different scaffolds were used. These scaffolds were essential for conducting a complete assessment of the entire impacted location and ensuring that a variety of orientations and directions were covered. This approach provided a holistic view of the disease's impacted site. The process of segmenting DICOM image files into different regions of interest from CBCT scans subsequently generating a 3D model depicting the patient's jaw anatomy for analysis in the context of patient-specific periodontitis is shown in Fig. 1.

We started with DICOM data, which we extensively preprocessed to remove any noise and artifacts so that we could begin delving into the complexity of our research. This key step improved the image quality and established the groundwork for later precise segmentation. To increase the accuracy of our segmentation, we aligned numerous CBCT images, as shown in Fig. 1(a), as well as other imaging modalities to make sure everything was spatially consistent. Fig. 1(b) illustrates the importance and criticality of selecting a region of interest (ROI). This choice served as our guidance in extracting the structures necessary for the forthcoming model by indicating the precise region of the CBCT scan to be segmented. Each segmentation, was a step toward clarity, establishing the perimeters of our focus within the ROI. The segmented data eventually transformed into a 3D model, as seen in Fig. 1(c), marking the end of this step. This model wasn't merely a representation; whether a surface mesh or a volumetric portrayal was chosen, it served as a starting point for more in-depth research and understanding.

Computed tomography (CT) scans play a crucial role in medical imaging, providing detailed anatomical information (Gunn et al., 2021). One of the primary reasons for the growing popularity of dental CBCT (Cone Beam Computed Tomography) is its ease of use, which can be linked to its compact imaging range, low radiation dose, low cost, and simple operation (Sluimer et al., 2006). With an emphasis on the maxillary and mandibular areas, this study provides a comprehensive framework for improving CT scan analysis. It exhaustively details the procedures and materials utilized to expedite the process, with the goal of considerably improving image evaluation accuracy and efficiency.

#### 2.1. CT scan simplification/CT scan refinement and modeling

#### 2.1.1. Software selection and model refinement

3D Slicer modeling software was used in the first stage, which was a critical step in making it easier to read CT scans by emphasizing anatomical landmarks (Patel et al., 2019). Professionals navigating the complexity of the human anatomy without intrusive treatments will greatly benefit from this visualization's complexity.

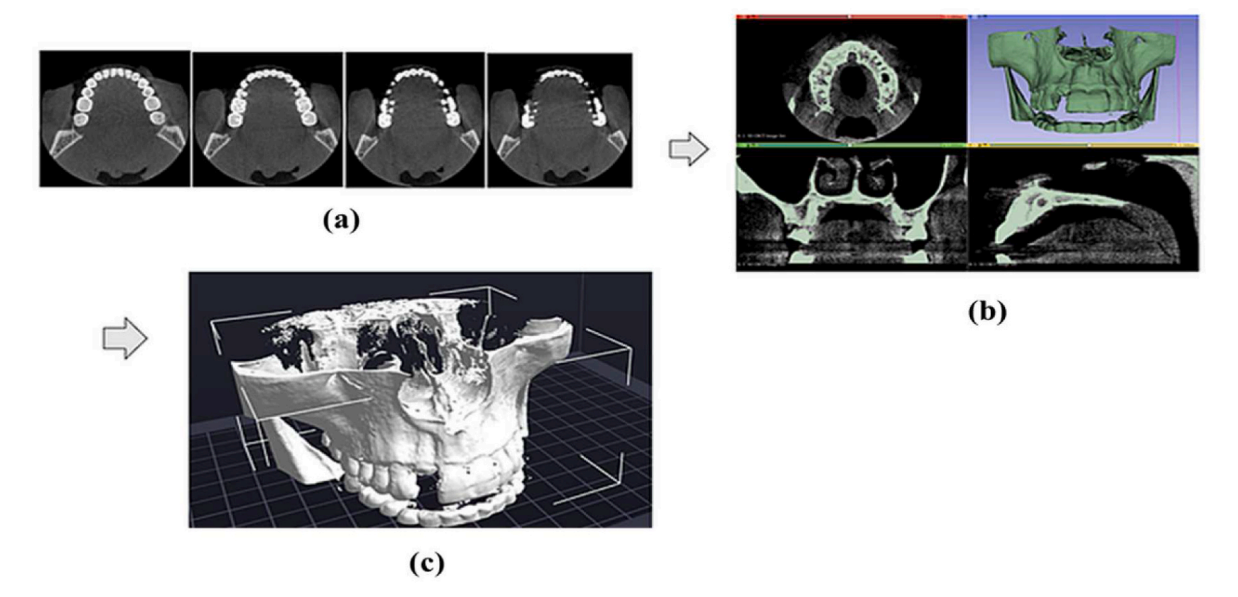


Fig. 1. (a) CBCT scans showcasing the patient's axial palatal view, (b) 3D modeling of the patient's dental anatomy derived from axial palatal CBCT scans, (c) Segmented 3D model of patient's diseased site.

# 2.1.2. Restoration of damaged bone regions using the Freeform Geomagic treatment method

The use of the innovative Freeform Geomagic software for the regeneration of damaged bone structures significantly enhanced the design process. The creation of precise designs required interdisciplinary cooperation between specialists and medical professionals. A 3D bone anatomy model that was created using accurate CT medical imaging data was imported into the Freeform Geomagic software to start the entire process. The model was transformed into a solid format to maintain structural integrity (Proksch and Galler, 2018). The ROI was then covered with a generous amount of moldable wax, creating a supporting structure. Using a specialized heated tool, the wax was carefully molded into the required scaffold design, enabling the creation of custom scaffold designs.

#### 2.2. Materials data

#### 2.2.1. Material selection

Numerous factors were carefully considered to ensure that the materials used would not only be functional but also safe for the user's health. Biocompatibility, the ability of a substance to interact with the body without having any negative effects, was one of the key problems (Ciani et al., 2016). To ensure that the constructed structures could withstand the forces applied to them, the mechanical features of the materials, such as their strength, were also taken into account (Camasão and Mantovani, 2021). Another important consideration was the biodegradability of the materials, as this would affect how long the constructed structures would last (Rezvani Ghomi et al., 2021).

#### 2.2.2. Expert collaboration

To gather crucial expertise in material selection, experts in biomaterials, dentistry, and materials engineering were engaged. Making rational choices about the optimal materials for the Maxilla, Mandible, and scaffold required gathering vital material data.

#### 2.3. Finite element analysis (FEA)

For carrying out the finite element analysis (FEA), the Mandible, Maxilla, and respective scaffold assemblies were imported to the ANSYS workbench. On analyzing the complexity of the geometry, it was found that the best element shape suited for the purpose is tetrahedral

elements (SOLID187), as they are efficient enough for static structural study with accurate results (Kladovasilakis et al., 2023). Furthermore, given that the smallest edge size was 0.1012 mm, adaptive meshing was employed to cover the complex geometry with a minimum mesh size was 0.02 mm. The total number of nodes and elements was 49,019 and 27,509, respectively.

#### 2.3.1. Material properties

To acquire the essential data on material properties, a detailed survey of previous studies was conducted. As bone analogs, the Maxilla and Mandible were mimicked, and their qualities were chosen to closely resemble their actual contacts and mechanical responses (Scocozza et al., 2023). All surfaces of the Maxilla, Mandible, and scaffold were rigorously prepped prior to simulations, eradicating any defects or extraneous factors that could impair contact precision.

#### 2.4. Boundary conditions

Boundary conditions were used in this study to both replicate the natural mastication process and to guarantee the stability and reliability of the analysis. The upper surface nodes of the Maxilla bone were first subjected to a fixed support restriction to limit translation and rotation. It is akin to the real-life constraint where the maxilla serves as a reference point. Whereas The mandible is fixed in the X and Z directions, emulating anatomical restrictions that limit lateral and anteriorposterior movements. This restriction is consistent with the physiological constraints observed in the human jaw. The mandible is left free to move in the Y direction. This freedom is reflective of the natural mobility of the mandible in the vertical plane, allowing for realistic articulation between the maxilla and mandible. Linear Displacement of the Maxilla: To replicate the conditions when the maxilla and mandible come into contact, the maxilla is subjected to linear displacement. This displacement is carefully applied to simulate the movement of the maxilla toward the mandible, mimicking the natural interaction between the two anatomical structures. The scaffold's rigidity and immobility during natural mastication were achieved by anchoring the maxilla bone. This restriction guarantees that the scaffold stays securely fixed to the Maxilla bone and for a precise evaluation of its mechanical reaction.

#### 3. Theory

A vertical force of 100 N was applied to the anatomy of the mandible to simulate the forces experienced during natural mastication. The load placed on the scaffold because of the vertical movement caused by biting or chewing is represented by this force. Based on physiological aspects of mastication and parameters like bite force or mastication (Zhao et al., 2023). In case of mastication condition, normal forces are applied over the surface of the targeted region, specifically at the incisor teeth. In this condition, the normal force of 100 N–130 N is directed at a 45-degree angle to the horizontal reference plane, simulating the natural masticatory forces during the biting process. In the case of the maxilla, the applied force acts in an outward direction and is equal and opposite to the force applied on the mandible, ensuring a balanced loading condition

To ensure symmetry and balance in parafunctional activities, forces ranging from 500 N to 530 N are applied at a 45-degree angle to the horizontal plane at the incisor teeth in both the maxilla (outward) and mandible (inward). This mimics parafunction—tightening and grinding of teeth—which puts additional strain on dental tissues above and beyond what occurs during regular mastication. The increased load from parafunctional activities can have a substantial impact on the long-term structural integrity and functionality of dental restorations and implants, hence it is imperative to acknowledge these increased forces when developing dental materials and scaffolds.

In trauma conditions, the normal load of 800 N is applied on both the maxilla and mandible incisor region at a 90-degree to the surface acting inward direction, representing an altered and potentially damaging loading scenario. This specific direction is chosen to simulate the unique loading patterns associated with traumatic events. A force of 800 N was applied at a  $90^{\circ}$  angle to the horizontal axes of the mandible and maxilla to mimic the trauma situation. This loading was designed to mimic a traumatic occurrence, such as a direct hit caused by an excessive amount of external force. The simulation considered the possible danger connected with the traumatic phases by applying the force under traumatic conditions to the maxilla and mandible. Clinical expertise and academic research served as the foundation for the forces and angles chosen for each loading situation (Poiate et al., 2009). To evaluate the periodontal scaffold model's structural response and identify any potential regions for stress concentration and deformation, these conditions were implemented.

#### 4. Results & discussions

To model the human jaw's mastication process, remote forces were applied on the Mandible and Maxilla regions using the simulation tool ANSYS Workbench. These forces represent the external loads experienced by the Mandible during chewing.

Upon selection of the designated component, the remote forces were defined in the external load section of ANSYS Workbench, in conjunction with the chosen component. The magnitude, direction, and point of application of the force were specified based on literature and pilot studies. Forces were applied evenly throughout the indicated elements, producing different conditions to replicate the various forces experienced during masticatory actions. The forces applied during the opening and closing portions of the mastication cycle were divided into three categories: mild (100-130 N), moderate (500-530 N), and high (800-830 N). A detailed assessment of the applied forces was performed to corroborate the model's accuracy. This was done to ensure that they were precisely put on the designated region of the Mandible, essentially mimicking the external loads that occur during the chewing process. Additional critical boundary conditions, such as fixed supports for the Maxilla and moment constraints on Mandible components, were imposed to allow precise modeling of anatomical motion.

During post-simulation in ANSYS Workbench, the findings were assessed to ascertain the Mandible's behavior in response to the imposed

remote forces. To understand the mechanical performance of the mandible when subjected to mastication forces, critical variables such as deformation magnitude and stress distribution assessments were examined.

Fig. 2 shows the segmented model with the objective to verify its accuracy and usability by precisely examining the affected regions. The measured dimensions for mandibular implants were observed to be 21.5  $\times$  11 mm, while Maxilla implants exhibited slightly smaller dimensions of 19.6  $\times$  13.2 mm. The implant covering one maximal incisor tooth in both the Maxilla and Mandible regions is 2.6 mm.

Fig. 3 (a) and Fig. 3 (b) show the assessment of anatomical fidelity during the design of wax models over the Mandible and Maxilla regions. The attention is placed on the evaluation of the accuracy and realism of the wax model in replicating the intricate anatomical features of the Maxilla and Mandible. This allows for insights into the capacity of Geomagic Freeform software to accurately represent complex anatomical structures, contributing to advancements in the development of more precise and patient-specific dental prosthetics and treatment planning.

Several challenges were faced while assembling parts in SolidWorks. Interference and clearance issues such as mate and alignment were encountered to ensure that the parts do not collide or have sufficient space, particularly in complex assemblies like Maxilla and Mandible as shown in Fig. 4 A and B. Mating and properly aligning parts proved to be challenging due to complex geometries and assemblies having numerous components Fig. 4(C). Design modifications in assemblies had an impact on connected components and made it harder to update them while retaining their right mating relationships.

The rationale is that bone, by utilizing its inherent qualities, accurately mimics the mechanical characteristics of these craniofacial regions. This decision improves simulation accuracy and provides a more accurate representation of biomechanical responses in the actual world under diverse settings (Herford and Boyne, 2008). It enables a more refined depiction of the mechanical reactions of these structures exhibited under an array of loading scenarios (Rasperini et al., 2015). Importantly, the complex structural behavior of the maxilla and mandible in these simulations is profoundly influenced by bone's anisotropic properties, which dictate that its mechanical responses differ according to the direction of the applied forces. Key bone properties elastic modulus, density, and Poisson's ratio are enumerated in Table 1. Our FEA models, designed with precision, quantify pivotal responses, including principal and Von Mises stresses, equivalent stress, and strain distribution in Maxilla and Mandible scaffolds under varied loads. Employing bone significantly elevates clinical applicability, refining accuracy in dental implant crafting and maxillofacial surgical planning by forecasting structural responses to diverse stressors while affirming integrity.

To accurately model the interaction between the scaffolds in Mandible and Maxilla in ANSYS, various stages must be methodically executed. It started with a complete import of the 3D models for both the scaffolds, making sure they were appropriately positioned and aligned. The mesh quality was critical for accurately representing the complicated shapes of the components. The distinct mechanical properties pertaining to the Mandible and Maxilla and the scaffold were determined once the geometric models were in place, capturing the specific biomechanical features of each. The defining of the interface interactions between the scaffold and the mandible, as shown in a referred Fig. 5, was a crucial step. As seen in Fig. 6, a bonded contact was chosen to provide a stable connection, and the interface regions were rigorously marked to determine the surfaces that would be in the immediate close by. The mesh's configuration was particularly vital; we employed an adaptive mesh pattern to balance computational efficiency with the necessity to capture critical anatomical nuances. This approach allows us to dynamically refine the mesh in specific regions with intricate details, ensuring that the simulation captures the nuances of the scaffold geometry effectively. The adaptability of the mesh enables us to focus

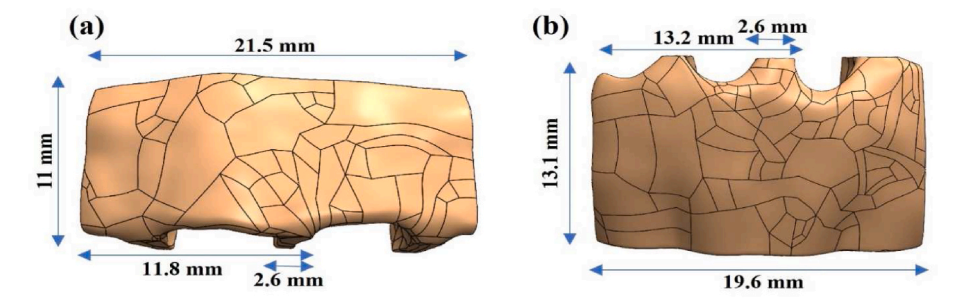


Fig. 2. Accurate assessment of affected Regions, (a). Individual scaffold measurement for Maxilla (b). Individual scaffold measurement for Mandibular joint.

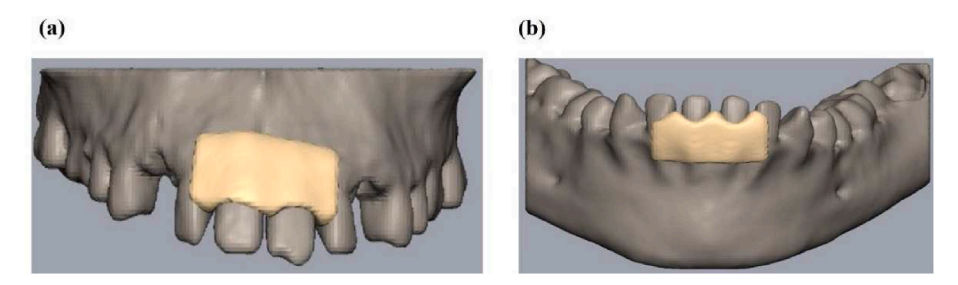


Fig. 3. A Wax model for scaffold in Freeform Geomagic over (a) Maxilla (b) Mandible.

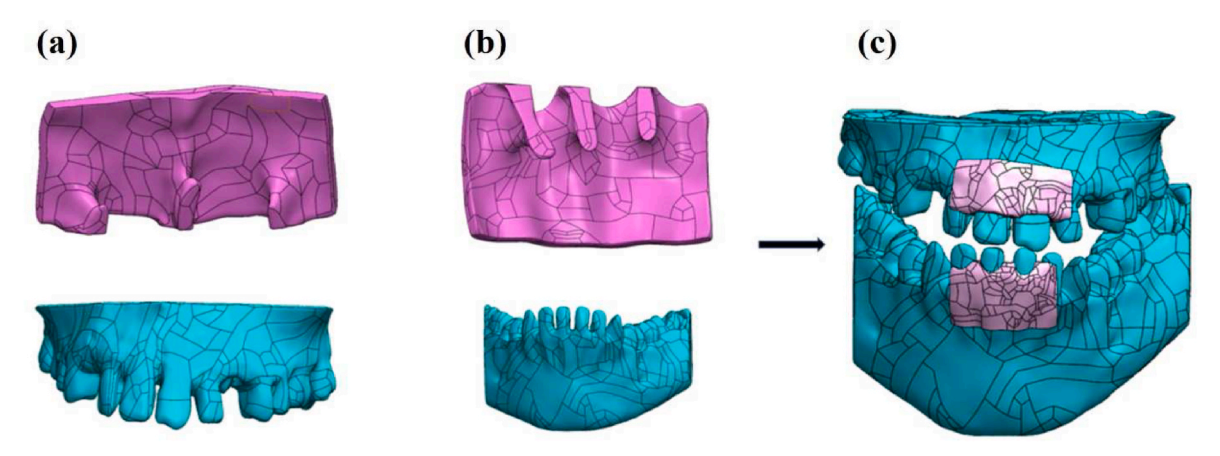


Fig. 4. (a) Maxilla region with scaffold placed exactly at the diseased site. (b) Mandibular region with scaffold placed exactly at the diseased site. (c) Completely assembled model in SolidWorks.

Table 1
Structural Properties considered for the Maxilla, Mandible and PCL Implant material (Poiate et al., 2009) (Schwitalla et al., 2015) (Rubo and Capello Souza, 2010) (Tribst et al., 2021).

Materials and properties	Maxilla (Bone) Structural properties	Mandible (Bone) Structural properties	PCL (Polymer) Structural properties
Density	1600 kg/m <sup>3</sup>	1600 kg/m <sup>3</sup>	1300 kg/m <sup>3</sup>
Young's	1.35 e <sup>+10</sup> Pa	1.55 e <sup>+10</sup> Pa	1 e <sup>+08</sup> Pa
Modulus			
Poisson's	0.3	0.3	0.44
Ratio			
<b>Bulk Modulus</b>	1.125e <sup>+10</sup> Pa	1.2917 e <sup>+10</sup> Pa	2.7778 e <sup>+08</sup> Pa
Shear	5.1923 e <sup>+09</sup> Pa	5.9615 e <sup>+09</sup> Pa	3.4722 e <sup>+07</sup> Pa
Modulus			

computational resources where they are most needed, optimizing the balance between accuracy and computational efficiency.

Regarding the perceived low-accuracy implications attributed to the number of nodes and tetrahedral elements, we would like to emphasize that the tetrahedral elements were chosen based on the intricate nature of the scaffold geometry. While tetrahedral elements (SOLID187) are known for their versatility in handling complex geometries, we acknowledge that their accuracy can be sensitive to mesh size and aspect ratio. Our mesh size selection, guided by adaptive techniques, aims to address these concerns by refining the mesh in critical regions. To ensure computational accuracy, we have conducted a thorough mesh sensitivity analysis to validate the mesh's appropriateness for our simulation objectives. We have implied the adaptive meshing strategy, along with careful consideration of optimized mesh parameters, providing balance between accuracy and computational efficiency.

With a minimum edge size of 0.1012 mm, our mesh comprised 27,509 quadratic tetrahedral elements and 49,019 nodes, as detailed in Fig. 7. Mesh convergence, especially at the junctures between the Maxilla and Mandible, posed significant challenges, often demanding iterative refinement for accuracy.

Such analysis yielded insights into tooth alignment under varying biting conditions and enabled evaluation of the impact on adjacent structures, substantiating the mesh's utility and reliability for subsequent, detailed simulations.

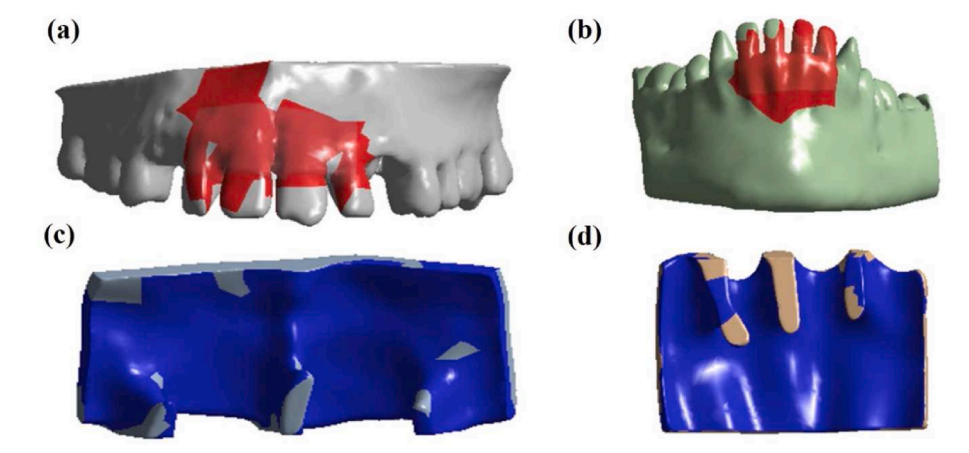


Fig. 5. Contact conditions between the scaffold and the bone. Contact between A Maxilla-scaffold B Mandible-scaffold C Maxilla's scaffold D mandibular Scaffold.

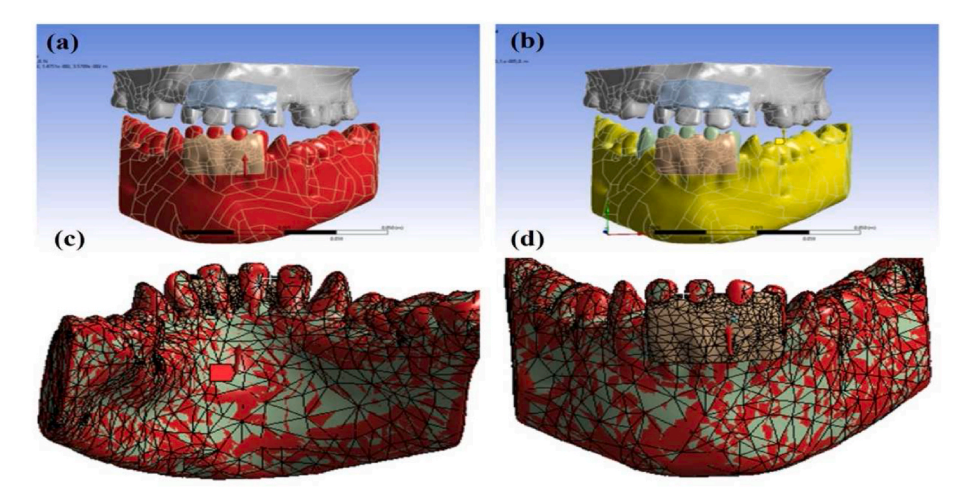


Fig. 6. (a) The force being applied at the Mandible and with the complete anatomy (b) The displacement occurred at the Mandible due to the forces applied (c) the application of force in the vertical direction on the Mandible (d) distribution of force in the whole geometry.

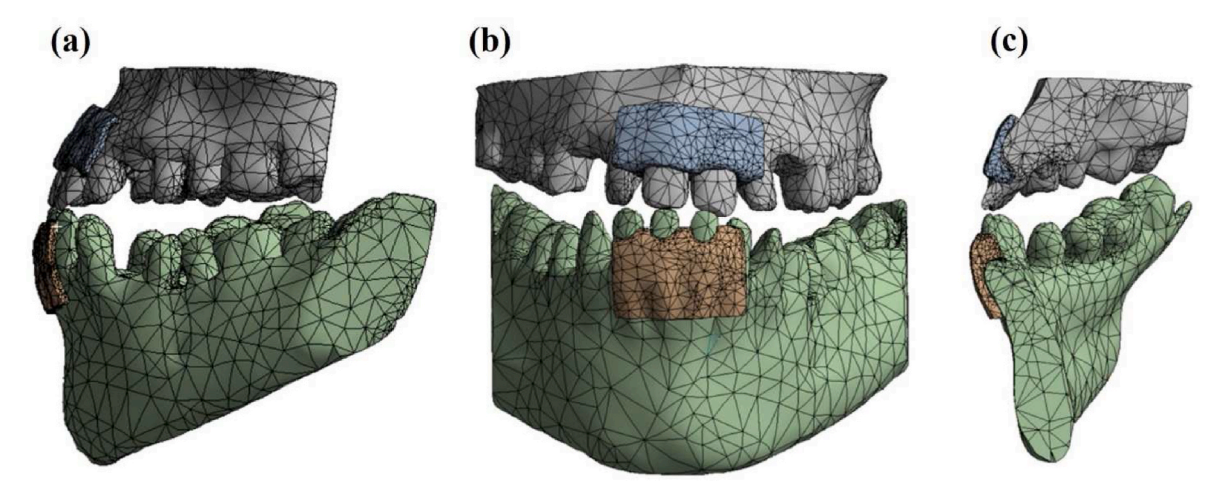


Fig. 7. Meshing the whole geometry before simulation (a) Side view (b) front view and (c) sectional view.

Fig. 8 illustrates the forces of natural mastication, such as chewing on the Mandibular and Maxillary scaffolds. The highest principal tensile stress applied to the scaffold above the Maxilla, as shown in Fig. 8 (a) and Fig. 8 (b), is 1.3562 MPa, while the compressive stress applied to the scaffold is -0.21203 MPa. It is the front of the scaffold where most of the

compressive stress is distributed. The principal primary strain obtained by natural mastication is 0.0020 MPa, which is well below the permitted limit. The front end of the scaffold experienced the least amount of compressive strain. The scaffold's connection to the Maxilla is subjected to an overall compressive stress in a range of -0.03778 MPa-0.31072

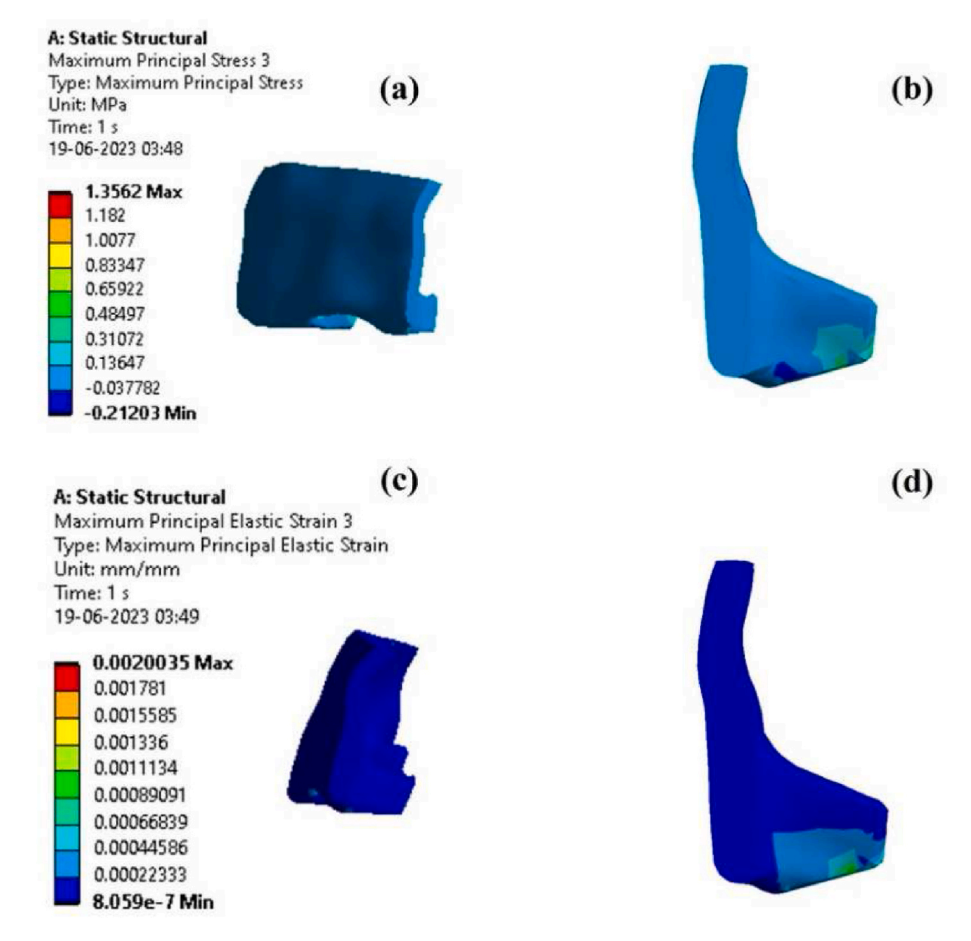


Fig. 8. Evaluation of (a, b) maximum principal stress and (c, d) maximum principal strain developed due to normal mastication forces applied on the Maxilla scaffold (b) stress distribution in the scaffold (d) strain distribution in the scaffold.

MPa, as shown in Fig. 8 (c). Similarly in Fig. 8 (d), the Maxilla-related scaffold experiences a minimum strain of  $8.059 \times 10^{-7}$ . Thus, when only natural mastication takes place, the principal stresses and strains on the scaffold remain within the range of the minimum permissible compressive stress and strain, with most of the compressive stress distributed at the front end of the structure.

Following a detailed analysis of the stress distribution in the scaffold under occlusal loading, it can be noted from Fig. 9 (a) and (b) that a maximum tensile stress of 6.896 MPa and a maximum principal strain of 0.01286 are generated. The buccal region of the scaffold experienced the highest level of stress and strain, while the palatal surface underwent a lower degree of stress and strain as shown in the figure. According to Fig. 9(c) and (d), the results refer to the parafunctional case where the maximum principal stress and strain were recorded as 33.942 MPa and 0.0627, respectively, indicating that the scaffold is under more stress and deformation based on the force in the range of 500-550 N applied at 45° to the Mandible. This result falls within the scaffold's elastic limits, indicating that the structure deforms elastically and quickly returns to its original shape after the stress has been released. During trauma cases, the buccal surface undergoes the highest degree of stress and tension, while the palatal surface experiences minimal force concentration as evident from Fig. 9 (e) and Fig. 9 (f). There is a noticeable increase in stress and strain when forces between 800 and 850 N are applied to the implant, with yield stress largely showing up at the buccal end of the tooth. Such force magnitudes can accelerate tooth displacement, possibly resulting in root resorption or other detrimental effects. The maximum principal strain was identified to be 0.0549, an indicator that the exerted load is within the scaffold's engineered thresholds. This data suggests the likelihood of elastic deformation, wherein the scaffold,

despite temporary deformation, reverts to its initial form post-stress. Internal stress concentration within the scaffold was mapped, extending from -22.82 to 20.479 MPa, while the buccal area endured a more pronounced strain, delineated between 2  $\times$  10 $^{-3}$  and 8.05  $\times$  10 $^{-7}$ .

These findings emphasize the imperative of detailed stress distribution scrutiny in scaffold design, crucial for averting unanticipated repercussions and guaranteeing results that align with patient oral health. Furthermore, the distinctive stress profiles experienced by load-bearing materials necessitate comprehensive examination, affirming both structural robustness and therapeutic effectiveness. Fig. 10 (a) and Figure (b) show that the forces are mostly acting in the section connected to the teeth, within the scaffold. This area exhibits elastic strain, indicating the reversible deformation of the scaffold material under the imposed forces. Further, the von Mises stresses developed must be compared with the stress limits to ascertain the possibility of failure of the material. There is no region in this instance where most of Von Mises stress experienced across the scaffold geometry fairly stays within the permissible limits, which do not exceed 0.46 MPa.

This study aids in locating key regions where stress concentrations might develop and result in failures. It should be observed that crossing over the material's elastic limit may cause the scaffold to irreversibly affect or become compromised. Moreover, persistent exposure to loads that are within the elastic range of the material can result in material fatigue, which could eventually lead to the gradual breakdown of the scaffold's structural integrity. During the mechanical analysis of PCL implants, it was realized that certain scenarios will produce both tensile and compressive forces. It was observed that the maximum tensile stress occurs at the upper edges of the L section 20.479 MPa, while the maximum compressive stress is encountered at lower section of L.

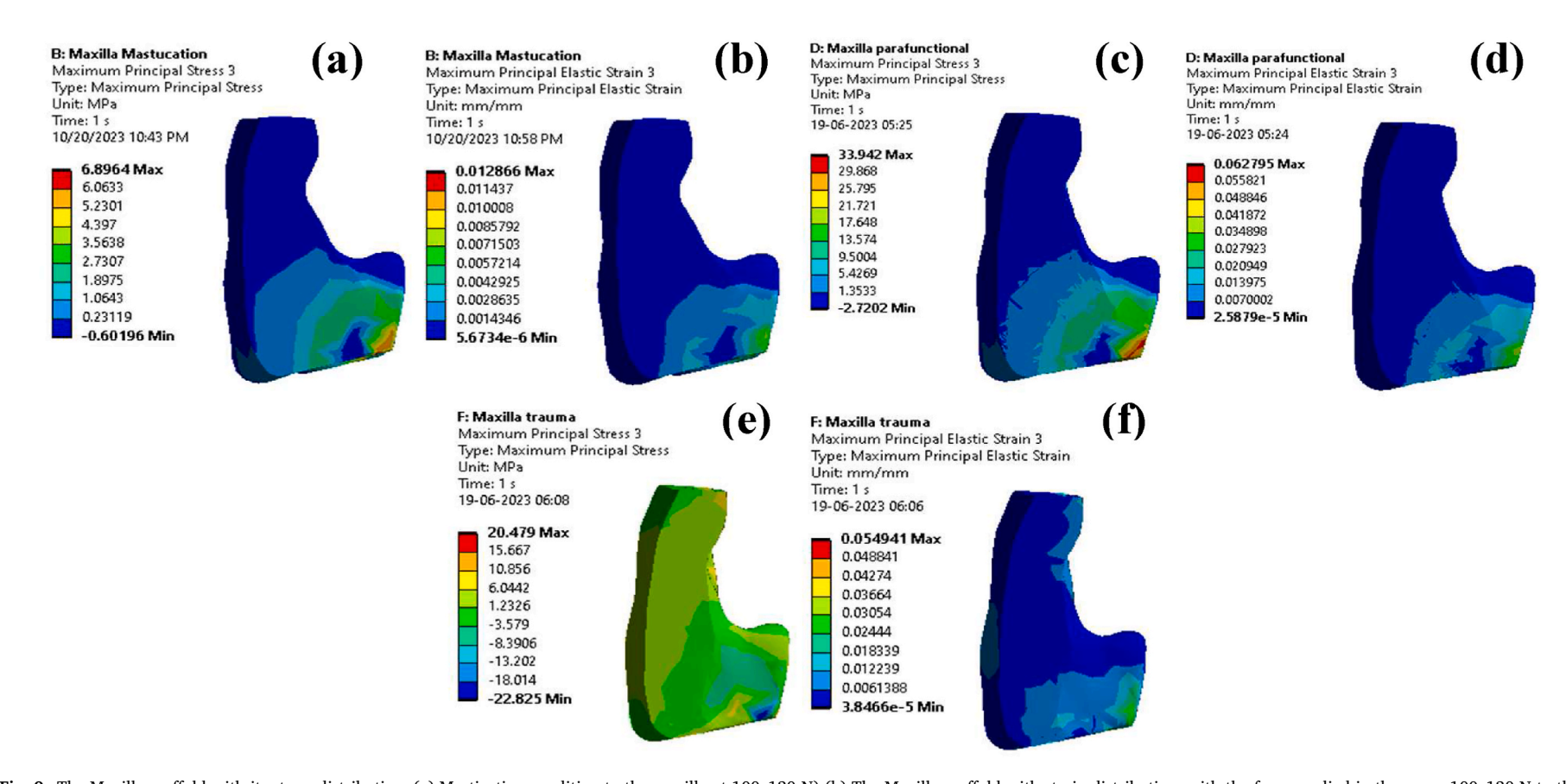


Fig. 9. The Maxilla scaffold with its stress distribution, (a) Mastication condition to the maxilla at 100–130 N) (b) The Maxilla scaffold with strain distribution, with the force applied in the range 100–130 N to the Mandible, (c) The Maxilla scaffold with its stress distribution and when the force applied is 500–550 N to the Mandible, (d) The Maxilla scaffold with its strain distribution when the force applied is 500–550 N to the Mandible, (e) The Maxilla scaffold with its strain distribution, when the force applied is in the range 800–850 N to the Maxilla.

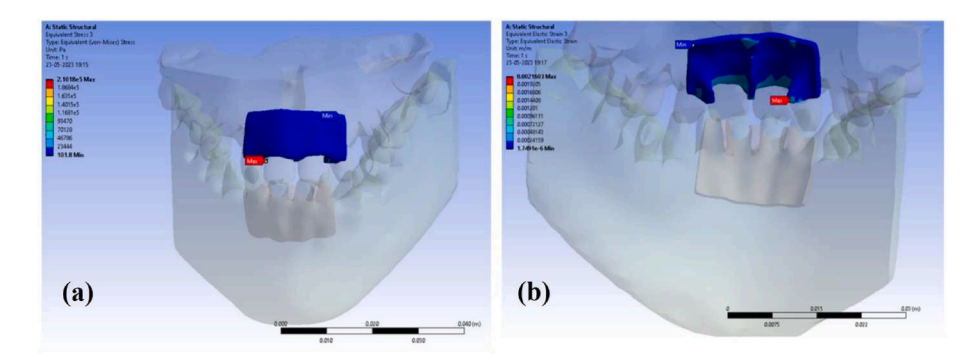


Fig. 10. (a) Equivalent von Mises stress acting in the Maxilla region. (b) Equivalent von Mises strain acting in the Maxilla region.

During simulation, the blue region of the scaffold is the area that is subjected to compression and is in contact with the bone area, while the green region is in contact with teeth and experiences tension. The red region, which experiences the highest levels of tensile stress, is a critical area of concern. Further, the mechanics of materials in the case of scaffolds are complex. For example, as shown in Fig. 9 the lower 'L' section of the scaffold is in contact with the gum from both inside and outside. This section will experience tensile forces at the bottom and compressive forces in the upper region. Similarly, as shown in Fig. 11 the 'P' section of the scaffold will be in contact with the teeth both from the inside and outside. This section will also experience tensile forces at the bottom and compressive forces in the upper region.

Fig. 11 (a) and (b) shows that in the case of natural mastication, a maximum tensile stress of 1.379 MPa and a maximum principal strain of 0.00216 is observed on the scaffold's front plane, which is significantly less than the allowed limit. According to Fig. 8 (a), the link between the scaffold and the Maxilla is under a compressive stress of -0.03778 MPa. The Maxilla-related structure in Fig. 8 (c) also receives a maximum strain of  $8.059\times10^{-7}$ . These results lead to the observations that when only natural mastication forces are applied to a scaffold, the stress-strain developed remains within the range of the minimum permitted compressive stress and strain, with most of the compressive stress and strain being distributed at the front end of the structure. Fig. 12 shows

the stress-strain distribution over the Mandible region of scaffold for different load conditions. Fig. 12 (a) shows that 12.545 MPa of principal tensile stress was exerted on the Mandible. The buccal region of the scaffold experienced the highest level of stress and strain, while the palatal surface underwent a comparatively lower degree of stress and strain. Fig. 12 (b) shows the principle elastic strain was 0.0182 which falls within the permissible elastic limits of PCL scaffold. This signified that the structure exhibited elastic deformation and promptly restored its original shape upon the release of stress. The stress and strain levels escalate significantly when forces ranging from 500 to 550 N are applied to the implant. It was observed that the yield stress was directed toward the teeth, primarily at the buccal end. Excessive force can cause the teeth to move too quickly, leading to root resorption or other forms of damage. Moreover, elevated levels of stress and strain can potentially cause pain and discomfort for the patient, which can significantly impact compliance with the treatment plan. From Fig. 12 (c) and (d), one can observe that a maximum principal stress of 41.31 MPa and a maximum principal strain of 0.05898 were imparted on the scaffold suggesting that even after the scaffold is experiencing an enormous amount of load there is only -5.780 MPa compressive stress that is being distributed at the mandibular bone region. The maximum tensile stress experienced in this case is on the teeth side. The external part of the scaffold demands a thorough inspection as there are no concentrated forces acting on it.

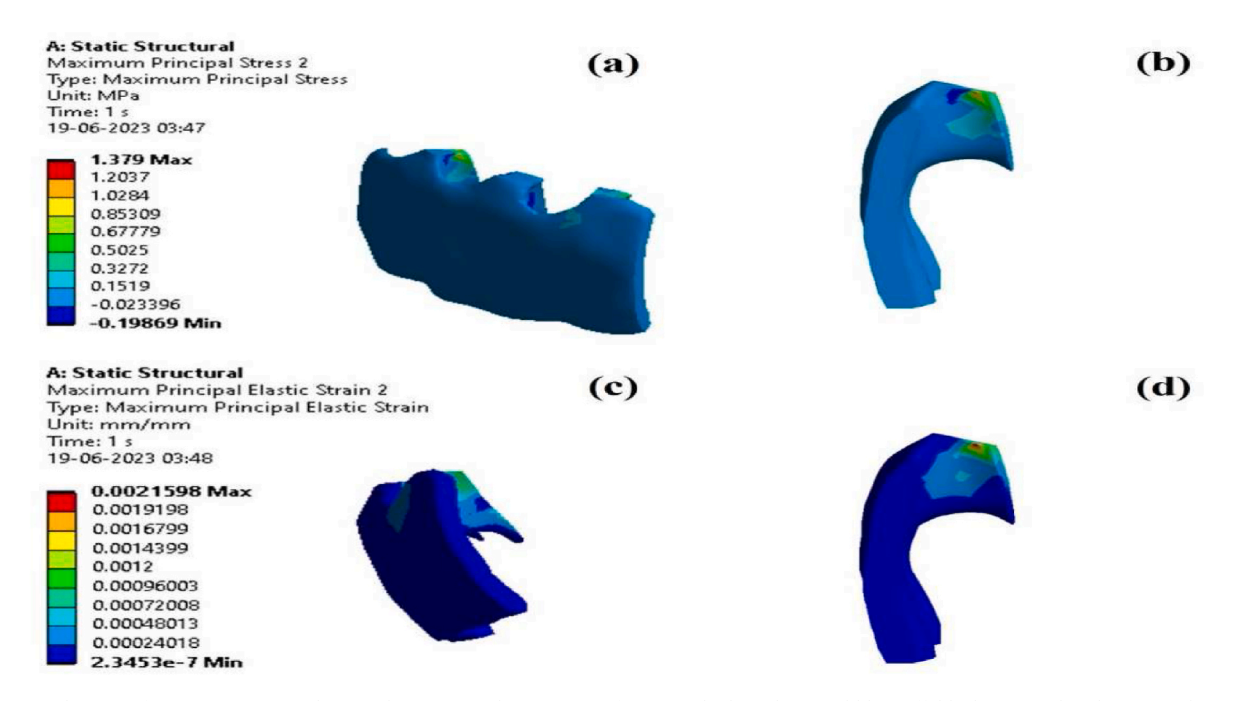


Fig. 11. (a) Evaluation of maximum principal stress due to normal mastication forces applied on the Mandible scaffold, (b) Stress distribution in the scaffold (c) maximum principal strain through normal mastication forces applied on the Mandible scaffold and (d) Strain distribution in the scaffold.

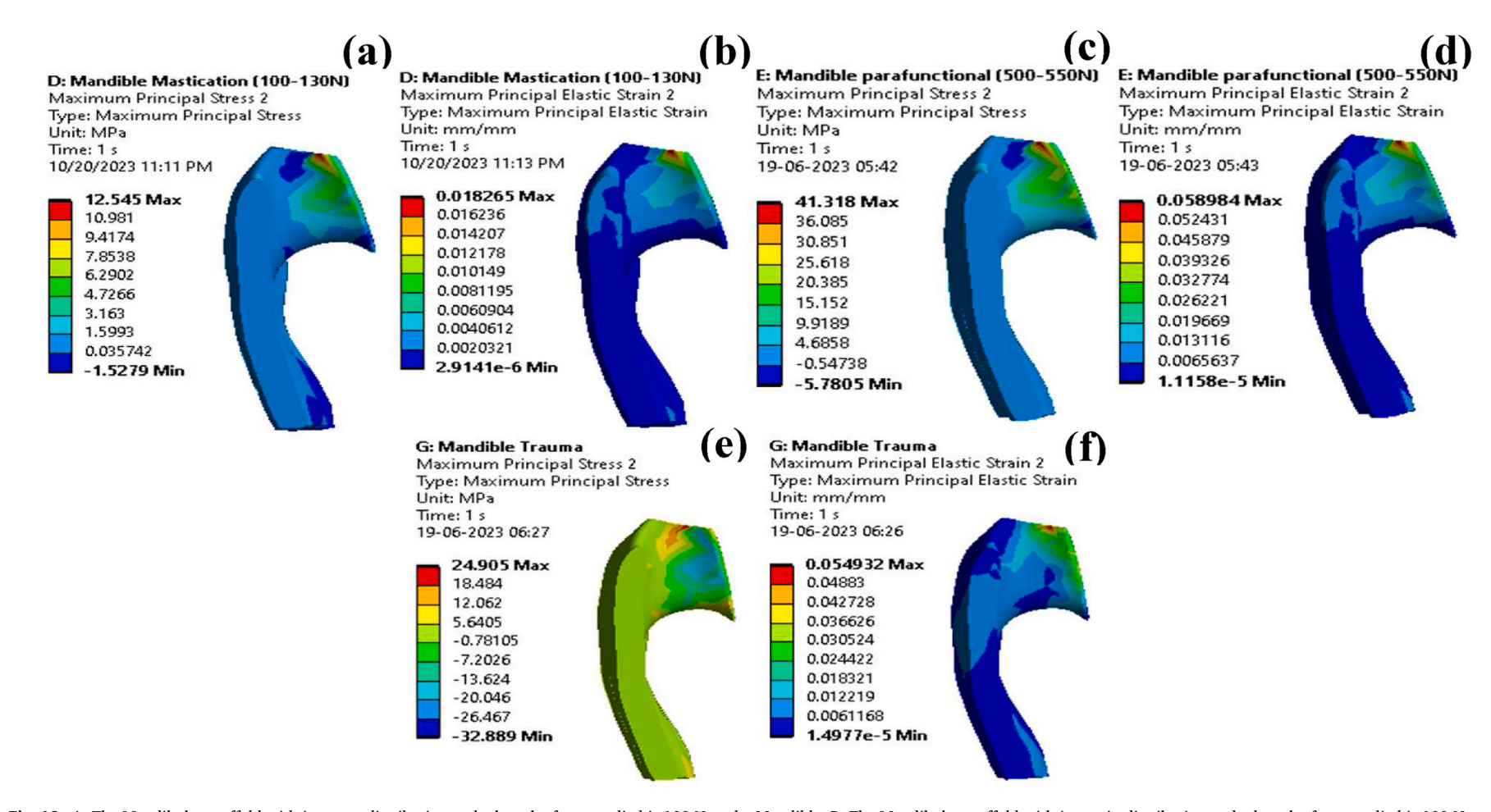


Fig. 12. A: The Mandibular scaffold with its stress distribution and when the force applied is 100 N to the Mandible. B: The Mandibular scaffold with its strain distribution and when the force applied is 500–550N to the Mandible. D: The Mandibular scaffold with its strain distribution when the force applied is 500–550N to the Mandible. E: The Mandibular scaffold with its strain distribution and when the force applied is 500–550N to the Mandible. F: The Mandibular scaffold with its strain distribution and when the force applied is 800–850N to the Mandible.

Overall Fig. 12 shows that mostly the forces are acting within the scaffold, primarily in the section connected to the teeth. This area exhibits elastic strain, indicating the deformation of the scaffold material under the imposed forces. The state under trauma is shown in Fig. 12 (e) and 12 (f) when a load of 800–850 N is applied; the stress imposed on the scaffold is 24.905 MPa. However, Fig. 12 (e) shows that most of the exterior part of the scaffold is distributed with a compressive stress ranging from -0.781 MPa to -7.21 MPa.

With a Von Mises stress value of 0.285 MPa, the scaffold successfully captured the stress profile across the structure under conditions of normal chewing, unusual functioning, and traumatic stress. An accurate evaluation of the scaffold's durability and load-bearing capability was made possible by the Von Mises criterion. A maximum Von Mises stress of 0.285 MPa and equivalent Von Mises strain of 0.00359, as shown in Fig. 13 (a) and Fig. 13(b), indicates the overall equivalent Von Mises stress of and strain state encountered in the scaffold and assessed the scaffold's potential for yielding or plastic deformation in viscoelastic materials.

Fig. 14 shows the intricate biomechanics of the maxillofacial region play a critical role in enduring various mechanical stresses encountered during different activities such as mastication, parafunction, and trauma. Understanding the stress distribution within the periodontal scaffolds of the maxilla and mandible under these diverse conditions is paramount, as it not only sheds light on their physiological adaptability but also underscores potential vulnerabilities that may necessitate clinical intervention.

#### 5. Discussion

Under natural masticatory conditions, the periodontal scaffolds in both the Maxilla and Mandible are subjected to minimal stress. This indicates the mechanical integrity and efficacy of the integrated compensating mechanisms that allow the mouth cavity to endure the regular stresses generated by daily motions like mastication. Specifically, the recorded tensile and compressive stresses within this context remain within the low range, suggesting that the physiological load during natural mastication is well within the tolerance limits of the periodontal structures. This finding reaffirms the concept that natural mastication forces are typically within the biomechanical competence of healthy periodontal scaffolding.

However, the situation alters when the oral structures are exposed to regulated mastication forces, particularly those between 100 N and 130 N. The scaffolds' stress increases significantly under these conditions. Both the mandible and the maxilla are subjected to significant amounts of stress; nevertheless, it is vital to note that the mandible has a more strong potential for adaptation, as seen by its greater tolerance to tensile stresses. This might be explained by the mandible's innate anatomical and biomechanical characteristics, which may provide it a higher

threshold against applied stresses than the maxilla.

Stress levels are noticeably increased in parafunctional settings, which are defined by the application of significantly higher forces (500 N–550 N). These circumstances can include bruxism or other dysfunctional habits that frequently place undue strain on the periodontium. The scaffolds in both areas experience much higher compressive and tensile loads, highlighting the possibility of pathological changes or damage when exposed to these intense forces. Interestingly, the Mandible nevertheless shows greater adaptability, even though the forces involved may exceed both structures' physiological tolerance levels.

The maxillofacial scaffolds experience specific and complex stress distribution due to traumatic events, particularly frontal impacts. Trauma produces a distinctive pattern that is defined by a raise in both tensile and compressive stresses, particularly when it involves direct impact to the fore teeth. Since substantial compressive stresses can cause a variety of periodontal injuries, such as fractures, dislocations, or other types of structural damage, it is especially concerning that in certain situations, compressive stress exceeds tensile stress. Results indicate a higher susceptibility in the mandibular front region, where the incisors and adjacent scaffolds carry most of the compressive stress. The difference in response between the maxilla and mandible becomes more pronounced as the stress range progresses from routine chewing to parafunctional activities and, finally, traumatic situations. While the mandible is more resistant to damage, it is worth noting that it experiences more stress, especially under strong strain circumstances. The need for protective measures is reiterated by this differential vulnerability, particularly in contact sports or other high-risk activities where the possibility of a frontal hit is increased. It is imperative to employ preventative measures like custom-fitted mouthguards since they can lessen the force of hits and possibly stop a chain reaction of tooth injuries.

The results show how periodontal scaffolds in the maxilla and mandible regions respond dynamically and with diverse adaptability to stresses that are both functional and non-functional. They also encourage further investigation into the biomechanical characteristics of these scaffolds, which may direct future research in the direction of the development of bioengineered scaffolds with improved stress tolerance, strengthening one of the most important functional systems in the human body.

#### 6. Conclusions

An in-depth study was carried out to examine the mechanical details of scaffold-bone interactions when employing Polycaprolactone (PCL) implants to regenerate new bone tissues. The investigation's thrust was to optimize the mechanical performance of PCL implants for effective periodontitis treatment. The study not only carried out simulations but

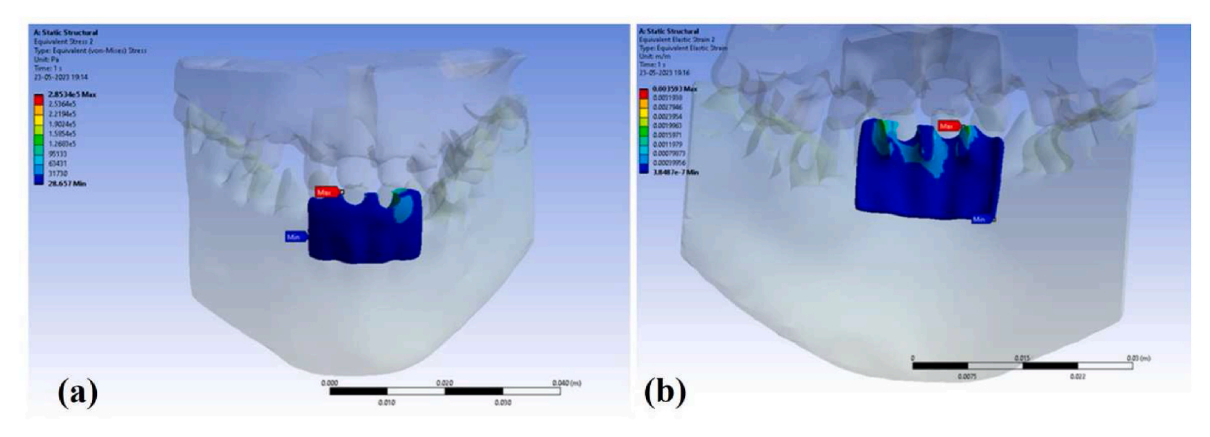
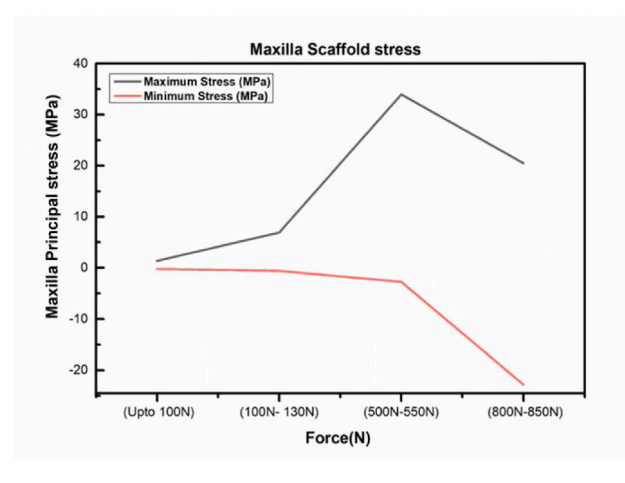


Fig. 13. (a) Equivalent von Mises stress, and (b) Equivalent von Mises strain values, acting in the Mandible region.



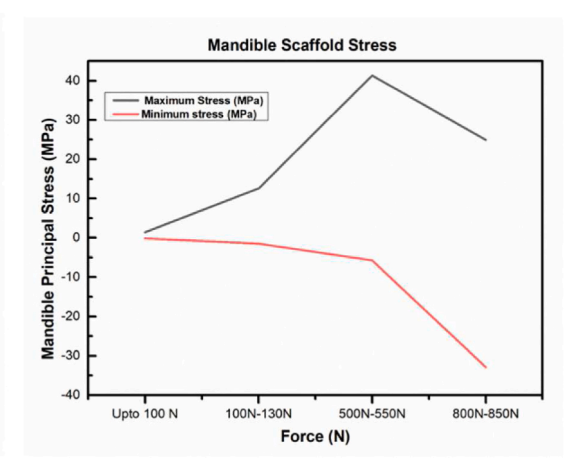


Fig. 14. (a) Maxilla scaffold stress (b) mandible scaffold stress.

also compared simulated results with empirical data, that helped in comprehending load distribution, displacement, and stresses developed. Significant technical challenges emerged during mesh generation. owing to the complex geometries, especially that of Maxilla and Mandible connections with their scaffolds. The adaptation of a mesh pattern led to enhanced simulation accuracy. The mesh was instrumental in correctly analyzing stress distribution, revealing potential vulnerabilities and deformation zones, vital for scaffold optimization. Another technical step was the assignment of distinct material properties to the Mandible and scaffold based on their inherent behavior. The precision with which material characteristics were defined was critical since it ensured that the simulations matched the real-world physics and responses of the materials in the problem. The study also used advanced finite element analysis to investigate the directional qualities of the bones in the jaw and upper mouth, offering information on the complicated nature of mandibular and maxillary bone structure. By applying constant elastic moduli in orthogonal orientations across the maxilla and mandible, this study leads the way in stimulating bone regeneration and has a major impact on scaffold design through Poisson's ratio. This method, which closely resembles the behavior of real tissues, marks a substantial advancement in tissue engineering. The article proposes a complete method for improving the interaction between scaffolds and bone utilizing PCL (polycaprolactone) implants, combining in-depth computational analysis with empirical data while taking individual biomechanical factors into account. The methods used in this study lay a solid foundation for the advancement of strategies in bone tissue regeneration and periodontal treatment. By using personalized, data-driven approaches, this study significantly contributes to the field of periodontal therapy.

#### Declaration of generative AI in scientific writing

In the crafting of this manuscript, the guidance provided underscores the differentiation between the writing process and the utilization of AI tools for data analysis and insights extraction. The authors utilized generative artificial intelligence (AI) and AI-assisted technologies, specifically for enhancing the manuscript's language clarity and readability. This application was executed under stringent human supervision and subsequent rigorous review, acknowledging the potential of AI to produce potentially erroneous, incomplete, or biased content that might sound authoritative. In line with Elsevier's AI policy for authors, no AI or AI-assisted technologies were attributed authorship or co-authorship, as such roles embody responsibilities inherently human.

#### Submission declaration and verification

The submission of this article attests that the research and content presented have not been previously published, barring instances such as abstracts, lectures, or academic theses as detailed under 'Multiple, redundant or concurrent publication'. It is further affirmed that this article is not currently under review for publication elsewhere. All coauthors concur with this submission, and the institutions or authorities responsible for the research have either tacitly or explicitly endorsed its publication. The authors commit that, upon acceptance, the article will not be published elsewhere in an identical format, regardless of the language or medium, without the explicit written consent of the copyright holder. In line with ensuring the originality of submissions, this article may undergo scrutiny through tools like Crossref Similarity Check and other software designed to detect duplications or breaches of originality.

#### Ethics in publishing

This research adheres to ethical guidelines in publishing and responsible conduct of research.

#### Use of inclusive language

This manuscript has been written using inclusive language to ensure diversity, respect, and equal opportunities.

#### Copyright information

All rights reserved. No part of this manuscript may be reproduced or utilized in any form without written permission from the authors.

#### Role of the funding source

Placeholder for funding source information.

#### Funding

This research was financially supported by National Science Foundation NSF EPSCOR OIA-2148653. The research was also bolstered by resources available to the PDPM IIITDM Jabalpur. Any statement, opinion, recommendation, or conclusions shared are those only of the authors and do not necessarily relay the official positions of the United States National Science Foundation (NSF).

#### CRediT authorship contribution statement

Rakesh Pemmada: Writing – review & editing, Writing – original draft, Validation, Methodology, Investigation, Formal analysis, Data curation, Conceptualization. Vicky Subhash Telang: Writing – review & editing, Writing – original draft, Validation, Software, Methodology, Investigation, Formal analysis, Data curation. Puneet Tandon: Writing – review & editing, Visualization, Validation, Supervision, Software, Resources, Methodology, Formal analysis. Vinoy Thomas: Writing – review & editing, Supervision, Project administration, Funding acquisition, Conceptualization.

#### Declaration of competing interest

The authors declare that they have no known competing financial interests or personal relationships that could have appeared to influence the work reported in this paper.

#### Data availability

No data was used for the research described in the article.

#### **Acknowledgements:**

Rakesh Pemmada acknowledges the CERIF Graduate Student Fellowship as part of FTPP Program (UAH/UAB) and UAB Blazer Fellowship from Graduate School for his stipend and tuition support. We extend our profound gratitude to Prof. Vinoy Thomas and Prof. Puneet Tandon for their invaluable insights and guidance throughout the course of this research.

#### References

- Anjum, S., et al., 2022. Electrospun biomimetic nanofibrous scaffolds: a promising prospect for bone tissue engineering and regenerative medicine. Int. J. Mol. Sci. 23 (16) https://doi.org/10.3390/ijms23169206.
- Batool, F., et al., 2018. Synthesis of a novel electrospun polycaprolactone scaffold functionalized with ibuprofen for periodontal regeneration: an in vitro and in vivo study. Materials 11 (4), 1–18. https://doi.org/10.3390/ma11040580.
- Bottino, M.C., Thomas, V., Janowski, G.M., 2011. A novel spatially designed and functionally graded electrospun membrane for periodontal regeneration. Acta Biomater. 7 (1), 216–224. https://doi.org/10.1016/j.actbio.2010.08.019.
- Bottino, M.C., et al., 2012. Recent advances in the development of GTR/GBR membranes for periodontal regeneration a materials perspective. Dent. Mater. 28 (7), 703–721. https://doi.org/10.1016/j.dental.2012.04.022.
- Camasão, D.B., Mantovani, D., 2021. The mechanical characterization of blood vessels and their substitutes in the continuous quest for physiological-relevant performances. A critical review. Mater. Today Bio 10 (March). https://doi.org/ 10.1016/j.mtbio.2021.100106.
- Cancedda, R., Giannoni, P., Mastrogiacomo, M., 2007. A tissue engineering approach to bone repair in large animal models and in clinical practice. Biomaterials 28 (29), 4240–4250. https://doi.org/10.1016/j.biomaterials.2007.06.023.
- Choi, S.E., Sima, C., Pandya, A., 2020. Impact of treating oral disease on preventing vascular diseases: a model-based cost-effectiveness analysis of periodontal treatment among patients with type 2 diabetes. Diabetes Care 43 (3), 563–571. https://doi.org/10.2337/dc19-1201.
- Ciani, O., Armeni, P., Boscolo, P.R., Cavazza, M., Jommi, C., Tarricone, R., 2016. De innovatione: the concept of innovation for medical technologies and its implications for healthcare policy-making. Heal. Policy Technol. 5 (1), 47–64. https://doi.org/ 10.1016/j.hlpt.2015.10.005.
- Corrales, L.P., Esteves, M.L., Vick, J. aime E., 2014. Scaffold design for bone regeneration. Journal of nanoscience and nanotechnology. J. Nanosci. Nanotechnol. 14 (1), 15–56.
- Dwivedi, R., et al., 2020. Polycaprolactone as biomaterial for bone scaffolds: review of literature. J. Oral Biol. Craniofacial Res. 10 (1), 381–388. https://doi.org/10.1016/j. jobcr.2019.10.003.

- Fallah, A., et al., 2022. 3D printed scaffold design for bone defects with improved mechanical and biological properties. J. Mech. Behav. Biomed. Mater. 134 (August), 105418 https://doi.org/10.1016/j.jmbbm.2022.105418.
- Gauthier, R., Jeannin, C., Attik, N., Trunfio-Sfarghiu, A.M., Gritsch, K., Grosgogeat, B., 2021. Tissue engineering for periodontal ligament regeneration: biomechanical specifications. J. Biomech. Eng. 143 (3), 1–13. https://doi.org/10.1115/1.4048810.
- Gunn, T., Rowntree, P., Starkey, D., Nissen, L., 2021. The use of virtual reality computed tomography simulation within a medical imaging and a radiation therapy undergraduate programme. J. Med. Radiat. Sci. 68 (1), 28–36. https://doi.org/ 10.1002/jmrs.436.
- Herford, A.S., Boyne, P.J., 2008. Reconstruction of mandibular continuity defects with bone morphogenetic protein-2 (rhBMP-2). J. Oral Maxillofac. Surg. 66 (4), 616–624. https://doi.org/10.1016/j.joms.2007.11.021.
- Kladovasilakis, N., et al., 2023. Development of biodegradable customized tibial scaffold with advanced architected materials utilizing additive manufacturing. J. Mech. Behav. Biomed. Mater. 141 (January), 105796 https://doi.org/10.1016/j. imbbm.2023.105796.
- Lacroix, D., Prendergast, P.J., 2002. A mechano-regulation model for tissue differentiation during fracture healing: analysis of gap size and loading. J. Biomech. 35 (9), 1163–1171. https://doi.org/10.1016/S0021-9290(02)00086-6.
- Marei, M.K., Saad, M.M., El-ashwah, A.M., El-backly, R.M., Al-khodary, M.A., 2009. EXPERIMENTAL FORMATION OF PERIODONTAL STRUCTURE AROUND TITANIUM IMPLANTS UTILIZING BONE MARROW MESENCHYMAL STEM CELLS: A PILOT STUDY, vol. XXXV.
- Patel, R., Lu, M., Diermann, S.H., Wu, A., Pettit, A., Huang, H., 2019. Deformation behavior of porous PHBV scaffold in compression: a finite element analysis study. J. Mech. Behav. Biomed. Mater. 96 (April), 1–8. https://doi.org/10.1016/j. jmbbm.2019.04.030.
- Poiate, I.A.V.P., de Vasconcellos, A.B., de Santana, R.B., Poiate, E., 2009. Three-dimensional stress distribution in the human periodontal ligament in masticatory, parafunctional, and trauma loads: finite element analysis. J. Periodontol. 80 (11), 1859–1867. https://doi.org/10.1902/jop.2009.090220.
- Proksch, S., Galler, K.M., 2018. Scaffold materials and dental stem cells in dental tissue regeneration. Curr. Oral Heal. Reports 5 (4), 304–316. https://doi.org/10.1007/s40496-018-0197-8
- Rasperini, G., et al., 2015. 3D-printed bioresorbable scaffold for periodontal repair.

  J. Dent. Res. 94 (X), 1538–1578, https://doi.org/10.1177/0022034515588303.
- Rezvani Ghomi, E., et al., 2021. The life cycle assessment for polylactic acid (PLA) to make it a low-carbon material. Polymers 13 (11), 1–16. https://doi.org/10.3390/ polym13111854.
- Roseti, L., et al., 2017. Scaffolds for bone tissue engineering: state of the art and new perspectives. Mater. Sci. Eng. C 78, 1246–1262. https://doi.org/10.1016/j. msec.2017.05.017.
- Rubo, J.H., Capello Souza, E.A., 2010. Finite-element analysis of stress on dental implant prosthesis. Clin. Implant Dent. Relat. Res. 12 (2), 105–113. https://doi.org/ 10.1111/j.1708-8208.2008.00142.x.
- Schwitalla, A.D., Abou-Emara, M., Spintig, T., Lackmann, J., Müller, W.D., 2015. Finite element analysis of the biomechanical effects of PEEK dental implants on the periimplant bone. J. Biomech. 48 (1), 1–7. https://doi.org/10.1016/j. ibiomech. 2014.11.017
- Scocozza, F., Di Gravina, G.M., Bari, E., Auricchio, F., Torre, M.L., Conti, M., 2023. Prediction of the mechanical response of a 3D (bio)printed hybrid scaffold for improving bone tissue regeneration by structural finite element analysis. J. Mech. Behav. Biomed. Mater. 142 (January), 105822 https://doi.org/10.1016/j. jmbbm.2023.105822.
- Sluimer, I., Schilham, A., Prokop, M., Van Ginneken, B., 2006. Computer analysis of computed tomography scans of the lung: a survey. IEEE Trans. Med. Imag. 25 (4), 385–405. https://doi.org/10.1109/TMI.2005.862753.
- Szabadi, E., 1996. Mechanical and microstructural properties of polycaprolactone scaffolds with 1-D, 2-D, and 3-D orthogonally oriented porous architectures produced by selective laser sintering. Br. J. Psychiatry 169 (SEPT.), 380–381. https://doi.org/10.1192/bjp.169.3.380b.
- Tribst, J.P.M., Dal Piva, A.M. de O., Ausiello, P., De Benedictis, A., Bottino, M.A., Borges, A.L.S., 2021. Biomechanical analysis of a custom-made mouthguard reinforced with different elastic modulus laminates during a simulated maxillofacial trauma. Craniomaxillofacial Trauma Reconstr. 14 (3), 254–260. https://doi.org/10.1177/1943387520980237
- Yoon, J., Lee, S.H., Jeong, Y., Kim, D.H., Il Shin, H., Lim, S.Y., 2020. A novel mandibular advancement device for treatment of sleep-disordered breathing: evaluation of its biomechanical effects using finite element analysis. Appl. Sci. 10 (13) https://doi. org/10.3390/app10134430.
- Zhao, Z., Wu, Z., Yao, D., Wei, Y., Li, J., 2023. Mechanical properties and failure mechanisms of polyamide 12 gradient scaffolds developed with selective laser sintering. J. Mech. Behav. Biomed. Mater. 143 (May), 105915 https://doi.org/ 10.1016/j.jmbbm.2023.105915.